

Specific Ion Pairing and Interfacial Hydration as Controlling Factors in Gemini Micelle Morphology. Chemical Trapping Studies

Yan Geng,[†] Laurence S. Romsted,^{*,‡} and Fred Menger[§]

Contribution from the Department of Chemical and Biomolecular Engineering, University of Pennsylvania, Philadelphia, Pennsylvania 19104, Department of Chemistry and Chemical Biology, Rutgers, The State University of New Jersey, New Brunswick, New Jersey 08904, and Department of Chemistry, Emory University, Atlanta, Georgia 30322

Received October 5, 2005; E-mail: romsted@rutchem.rutgers.edu

Abstract: Results from chemical trapping experiments in micellar solutions containing 1.5–5 mM aqueous solutions of three didodecyl dicationic dibromide gemini surfactants with different methylene spacer lengths (12-*n*-12 2Br where *n* = 2–4 CH₂ groups) gave quantitative estimates of the molarities of interfacial bromide (Br_m) and water (H₂O_m), the fractions of free and paired headgroups and counterions, and the net headgroup charge. These results are one of the most detailed compositional studies of an association colloid interface to date. Br_m increases and H₂O_m decreases as *n* decreases and the two cationic charges are closer together. The 12–2–12 2Br gemini (the only one of the three geminis known to form threadlike micelles) shows a marked increase in Br_m (from 2.3 to 3.6 M) and a decrease in H₂O_m (from 35 to 17 M) at the exceptionally low surfactant concentration in the vicinity of the previously reported sphere-to-rod transition or second cmc concentration. Rod formation occurs because of an increase in headgroup-counterion association and dehydration at the micelle surface that depend on both the free energies of hydration and specific ion interactions and surfactant and counterion concentrations. These and other recent chemical trapping results support a new model for the balance of forces controlling morphological transitions of association colloids. The hydrophobic effect drives the formation of headgroup-counterion pairs, which have a lower demand for water of hydration. Release of water permits tighter packing and formation of cylindrical aggregates.

Introduction

Chemical trapping results reported here support a new interfacial specific ion-pairing/hydration model that rationalizes the morphological transitions of dicationic gemini micelles and, by inference, ionic amphiphiles in general.

The hydrophobic effect, in which amphiphile tails minimize their contact with water, drives amphiphile aggregation. Balance is provided by the hydration interactions of headgroups and counterions in the micellar interfacial region. Chemical trapping results presented here and published earlier^{1–3} show that morphological transitions occur when headgroup-counterion pairs are formed and some water of hydration is released. Invoking ion pairing in dilute aqueous solutions may seem surprising at first. However, above the critical micelle concentration (cmc) of amphiphiles (typically 1–100 mM depending upon the amphiphile chain length, headgroup structure, and counterion type), interfacial headgroup and counterion concen-

trations are high, on the order of 1–3 M.^{4,5} At this concentration ion pairing is viable, even in water.

Sphere-to-rod transitions, sometimes called the “second cmc,” are known to occur with increasing amphiphile or counterion concentration,⁶ but the concentration associated with the transition depends on the amphiphile headgroup structure and the counterion type.^{3,7–12} Those factors that promote rod formation by ionic micelles, i.e., lower free energies of ion hydration, weaker H-bonding with water, and increased ion polarizability, are the same ones that promote ion-pair formation and solvent release.^{13,14} Headgroup/counterion association reduces the demand for ion hydration, and water is released into the surround-

[†] University of Pennsylvania.

[‡] Rutgers, The State University of New Jersey.

[§] Emory University.

- Geng, Y.; Romsted, L. S.; Froehner, S.; Zanette, D.; Magid, L.; Cuccovia, I. M.; Chaimovich, H. *Langmuir* **2005**, *21*, 562–568.
- Romsted, L. S. Interfacial Composition of Surfactant Assemblies by Chemical Trapping with Arenediazonium Ions: Method and Applications. In *Reactions and Synthesis in Surfactant Systems*; Texter, J., Ed.; Marcel Dekker: New York, 2001; pp 265–294.
- Soldi, V.; Keiper, J.; Romsted, L. S.; Cuccovia, I. M.; Chaimovich, H. *Langmuir* **2000**, *16*, 59–71.

- Mukerjee, P. *J. Phys. Chem.* **1962**, *66*, 943–945.
- Romsted, L. S. A General Kinetic Theory of Rate Enhancements for Reactions between Organic Substrates and Hydrophilic Ions in Micellar Solutions. In *Micellization, Solubilization and Microemulsions*; Mittal, K. L., Ed.; Plenum Press: New York, 1977; Vol. 2; pp 489–530.
- Jonsson, B.; Lindman, B.; Holmberg, K.; Kronberg, B. *Surfactants and Polymers in Aqueous Solution*; John Wiley & Sons: Chichester, 1998.
- Imae, T.; Abe, A.; Ikeda, S. *J. Phys. Chem.* **1988**, *92*, 1548–1553.
- Imae, T.; Ikeda, S. *Colloid Polym. Sci.* **1987**, *265*, 1090–1098.
- Imae, T.; Ikeda, S. *J. Phys. Chem.* **1986**, *90*, 5216–5223.
- Imae, T.; Kamiya, R.; Ikeda, S. *J. Colloid Interface Sci.* **1985**, *108*, 215–225.
- Ikeda, S. Salt-Induced Sphere-Rod Transition of ionic Micelles. In *Surfactants in Solution*; Mittal, K. L., Lindman, B., Eds.; Plenum: New York, 1984; Vol. 2, pp 825–840.
- Porte, G.; Appell, J. The Sphere to Rod Transition of CPX and CTAX Micelles in High Ionic Strength Aqueous Solutions: The Specificity of Counterions. In *Surfactants in Solution*; Mittal, K. L., Lindman, B., Eds.; Plenum Press: New York, 1984; Vol. 2, pp 805–823.
- Marcus, Y. *Ion Solvation*; John Wiley & Sons: Chichester, U.K., 1985.

ing aqueous domain. The resulting increase in interfacial counterion and reduction in interfacial water concentrations, which are quantified by our chemical trapping method, permit tighter packing into cylindrical morphologies. Spherical micelles, on the other hand, are favored when the hydration free energies of headgroups and counterions are stronger and the ions are less polarized, such that fully hydrated ions are more abundant. In summary, we demonstrate for the first time that aggregate morphology and specific ion pairing by gemini amphiphiles are intimately related.

Many other micellar properties also depend on headgroup structure and counterion type such as the cmc, aggregation number, and Krafft temperature,⁶ and catalysis of chemical reactions.^{15,16} Properties of ion specific electrodes,¹⁷ biomembranes and proteins,^{18–21} and ion-exchange resins,²² and polyelectrolytes and DNA²³ also depend on the nature of the surface charge group and counterion type and concentrations. Most comparisons of specific ion effects focus on counterion type, and counterion effectiveness generally follows a Hofmeister series;²⁴ i.e., the larger, more polarizable, less strongly hydrated counterions have greater effects on a particular property, the same factors that enhance ion pair formation. Traditionally, ionic effects on colloidal structure are attributed to Coulombic interactions, electrostatic repulsions between the charged headgroups of the amphiphiles that are mediated by water and screened by counterions in an electrical double layer.^{25,26} The shortcomings of this perspective have been identified repeatedly and center around specific ion effects that have not been successfully incorporated.^{27–29} Molecular dynamic simulations of micelles and bilayers show that a significant fraction of the counterions in the interfacial region are in direct contact with the headgroups without intervening water and that the number of these contacts depends on counterion type.^{30–32} Thus, our interfacial specific ion-pairing/hydration model has substantial literature precedence. Indeed, the varied structural motifs of micelles and other association colloids (spheres, rods,

lamellar, cubic, etc.) depend on the structure and hydrophobicity of the amphiphilic tail(s), as is well-known, but also on specific ion hydration, ion-pairing, and the release of water into the aqueous domain. To our knowledge, the concept embedded in our model, namely that morphological transitions occur because interfacial ion-pair formation and release of interfacial water are driven by the hydrophobic effect, has not been previously considered and is one of the main subjects of this paper.

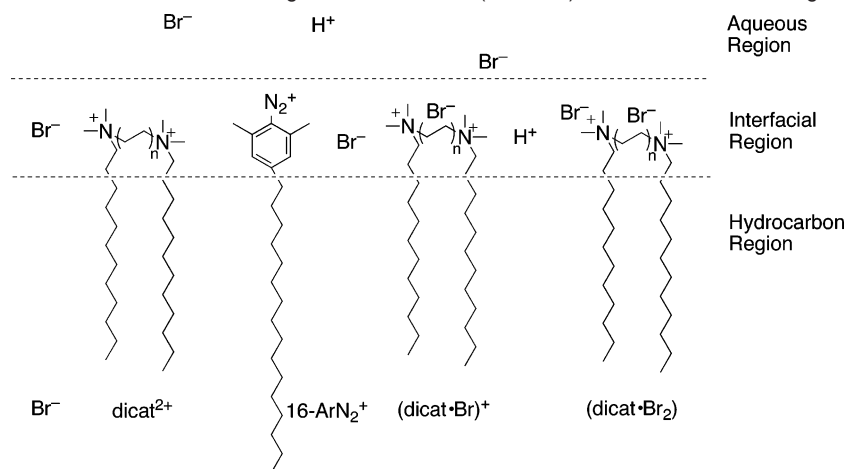
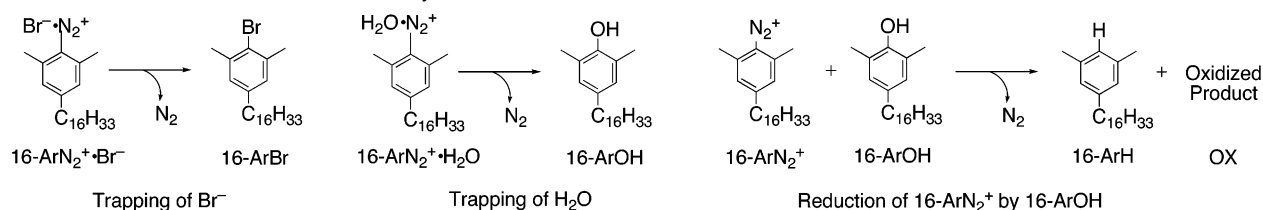
Gemini amphiphiles are receiving vast academic and industrial attention.^{33,34} They often form viscoelastic solutions, a form of “soft matter,”³⁵ because they readily form rodlike, threadlike, or wormlike micelles at very low concentrations and because their solution viscosities are “tunable” by changing the headgroup spacer length.³⁶ Potential applications, embodied in scores of patents and publications, include thickeners, drag reducers, oil well service fluids, heat and solid transfer agents, detergents, compounds for controlling aerosol droplet size,^{37–39} and gene transvection.⁴⁰

The three gemini surfactants used in these experiments differ only in spacer length and have about the same charge-to-hydrocarbon ratio or hydrophilic–lipophilic balance (HLB) as their single-chained analogue, $C_{12}H_{25}N(CH_3)_3^+Br^-$ (DTABr), but the properties of geminis and DTAB differ dramatically. The cmc values of the three geminis are about 1 mM,^{41,42} more than an order of magnitude smaller than the cmc of 14 mM for DTABr.⁴³ DTABr forms rodlike micelles only when the solution contains huge quantities of NaBr (1.8 M),⁴³ but 12-2-12 forms threadlike micelles in salt-free solutions at 4.2 mM.⁴⁴ Curiously, 12-3-12 and 12-4-12 micelles remain spheroidal up to much higher concentrations,^{34,45} yet reported values of the degree of counterion binding to the micelles (α) are not too different for all three surfactants: DTABr (0.20); 12-2-12Br (0.16); 12-3-12Br (0.21); 12-4-12Br (0.16, 0.26).^{41,44} Camesano and Nagarajan developed a thermodynamic model for the low cmc values of gemini surfactants, including spacer length effects,⁴⁶ but they did not consider the possibility ion-pairing and low hydration in the interfacial region.

Concomitant interfacial ion pairing and release of interfacial water also provides a sensible explanation for the markedly different effects of chloride and bromide ions on sphere-to-rod transitions of cetyltrimethylammonium micelles³ and the absence and presence of rod formation of cetyltrimethylammo-

- (14) Marcus, Y. *J. Phys. Chem. B* **2005**, *109*, 18541–18549.
 (15) Buntton, C. A.; Nome, F.; Quina, F. H.; Romsted, L. S. *Acc. Chem. Res.* **1991**, *24*, 357–364.
 (16) Savelli, G.; Germani, R.; Brinchi, L. Reactivity Control by Aqueous Amphiphilic Self-Assembling Systems. In *Reactions and Synthesis in Surfactant Systems*; Texter, J., Ed.; Marcel Dekker: New York, 2001; Vol. 100; pp 175–246.
 (17) Eisenman, G. *The Glass Electrode*; Interscience Reprint, Interscience: New York, 1965.
 (18) Diamond, J. M.; Wright, E. M. *Annu. Rev. Physiol.* **1969**, *31*, 581–646.
 (19) Collins, K. D. *Proc. Natl. Acad. Sci. U.S.A.* **1995**, *92*, 5553–5557.
 (20) Kirukhin, M. Y.; Collins, K. D. *Biophys. Chem.* **2002**, *99*, 155–168.
 (21) Cacace, M. G.; Landau, E. M.; Ramsden, J. J. *Q. Rev. Biophys.* **1997**, *30*, 241–277.
 (22) Reichenberg, D. Ion-Exchange Selectivity. In *Ion Exchange: A Series of Advances*; Marinsky, J. A., Ed.; Marcel Dekker: New York, 1966; Vol. 1, pp 227–276.
 (23) Record, M. T. J.; Zhang, W.; Anderson, C. F. *Adv. Protein Chem.* **1998**, *51*, 281–353.
 (24) Collins, K. D.; Washabaugh, M. W. *Q. Rev. Biophys.* **1985**, *18*, 323–422.
 (25) Hunter, R. J. *Foundations of Colloid Science*, 2nd ed.; Oxford: Oxford, 2001.
 (26) Israelachvili, J. *Intermolecular and Surface Forces*, 2nd ed.; Academic Press: London, 1991.
 (27) Kunz, W.; Lo Nostro, P.; Ninham, B. W. *Curr. Opin. Colloid Interface Sci.* **2004**, *9*, 1–18.
 (28) Bostrom, M.; Williams, D. R. M.; Ninham, B. W. *Phys. Rev. Lett.* **2001**, *87*, 168103–168104.
 (29) Manciu, M.; Ruckenstein, E. *Adv. Colloid Interface Sci.* **2004**, *112*, 109–128.
 (30) Faeder, J.; Albert, M. V.; Ladanyi, B. M. *Langmuir* **2003**, *2003*, 2514–2520.
 (31) Bockmann, R. A.; Hac, A.; Heimburg, T.; Grubmuller, H. *Biophys. J.* **2003**, *85*, 1647–1655.
 (32) Pandit, S. A.; Bostick, D.; Berkowitz, M. L. *Biophys. J.* **2003**, *84*, 3743–3750.

- (33) Menger, F. M.; Keiper, J. S. *Angew. Chem., Int. Ed.* **2000**, *39*, 1906–1920.
 (34) Zana, R.; Xia, J. *Gemini Surfactants: Synthesis, Interfacial and Solution-Phase Behavior, And Applications*; Marcel Dekker: New York, 2004; Vol. 117.
 (35) Zilman, A.; Tlusty, T.; Safran, S. A. *J. Phys.: Condens. Matter* **2003**, *15*, S57–S64.
 (36) Zana, R. *J. Colloid Interface Sci.* **2002**, *248*, 203–230.
 (37) Walker, L. M. *Curr. Opin. Colloid Interface Sci.* **2001**, *6*, 451–456.
 (38) Yang, J. *Curr. Opin. Colloid Interface Sci.* **2002**, *7*, 276–281.
 (39) Maitland, G. C. *Curr. Opin. Colloid Interface Sci.* **2000**, *5*, 301–311.
 (40) Kirby, A. J.; Camilleri, P.; Engberts, J. B. F. N.; Feiters, M. C.; Nolte, R. J. M.; Soderman, O.; Bergsma, M.; Bell, P. C.; Fielden, M. L.; Rodrigues, C. L. G.; Guedat, P.; Kremer, A.; McGregor, C.; Perrin, C.; Ronsin, G.; van Eijk, M. C. P. *Angew. Chem. Int. Ed.* **2003**, *42*, 1448–1457.
 (41) Menger, F. M.; Keiper, J.; Mbadugha, B. N. A.; Caran, K. L.; Romsted, L. S. *Langmuir* **2000**, *16*, 9095–9098.
 (42) Grosmaire, L.; Chorro, M.; Chorro, C.; Partyka, S.; Zana, R. *J. Colloid Interface Sci.* **2002**, *246*, 175–181.
 (43) Ozeki, S.; Ikeda, S. *J. Colloid Interface Sci.* **1982**, *87*, 424–435.
 (44) Bernheim-Groswasser, A.; Zana, R.; Talmon, Y. *J. Phys. Chem. B* **2000**, *104*, 4005–4009.
 (45) Danino, D.; Talmon, Y.; Zana, R. *Langmuir* **1995**, *11*, 1448–1456.
 (46) Camesano, T. A.; Nagarajan, R. *Colloids Surf. A Physicochem. Eng. Aspects* **2000**, *167*, 165–177.

Scheme 1. Cartoon Cross Section of the Interfacial Region of 12-*n*-12 2Br (*n* = 2–4) Gemini Micelles Showing the Ionic Components**Scheme 2.** Product Formation from the Heterolytic Dediazonation and Redox Reactions

nium micelles with 2,6- versus 3,5-dichlorobenzoate counterions, respectively.¹

Chemical Trapping

The logic and experimental protocols of the chemical trapping method are published,^{1–3,41,47–50} and only its specific application to gemini micelles is described here. The approach is grounded in the pseudophase model for chemical reactivity in micellar solutions.¹⁵ Scheme 1 illustrates a small section of the three regions in the immediate vicinity of the interfaces of aqueous gemini micelles: hydrocarbon core, interfacial, and aqueous. The cartoon illustrates the orientations of the amphiphilic arenediazonium ion probe, 4-hexadecyl-2,6-dimethylbenzene-diazonium ion (16-ArN₂⁺), and the free and paired headgroups and counterions. Scheme 1 also shows the symbols used to abbreviate these structures in the text. Bulk water and water of hydration are not shown. The three didodecyl tetramethyl dicationic dibromide geminis, 12-*n*-12 2Br, used in this study differ only in spacer length with *n* = 2–4 methylene groups. The first and second ion-pair association constants (defined below) for the formation of the monobromo (dicat·Br)⁺ and dibromo (dicat·Br₂) ion pairs, respectively, in water have already been estimated for bolaform salts, dicationic dibromo quaternary salts, 1-*n*-1 2Br (*n* = 2–4), that are structural models of the gemini headgroups, i.e., methyl groups instead of the dodecyl chains of the gemini surfactants.⁵¹ The association constants are numerically small, ranging from about 0.8–17 M⁻¹ (see

Discussion for individual values) indicating that the free energies of ion-pair formation are also small.

The distributions of components in the solutions of gemini micelles are assumed to be at dynamic equilibrium. Transfer rates of components between micelles are assumed to be orders of magnitude faster than the rate of the chemical trapping reaction (*t*_{1/2} about 90 min at 25 °C).² The reactive headgroup of 16-ArN₂⁺ is oriented in the interfacial region and its tail in the micellar core, Scheme 1, and product distributions from its reaction depend on the concentrations of components in the interfacial region. Perturbation of the micelle properties by 16-ArN₂⁺ is assumed to be minimal because: (a) the surfactant concentration is in 15–75-fold excess over 16-ArN₂⁺; (b) both the surfactant and the 16-ArN₂⁺ have identical charges; and (c) headgroup sizes of the gemini amphiphiles and probe are similar. Reaction is initiated by adding a small aliquot of 16-ArN₂BF₄ in CH₃CN to an aqueous micellar solution; the resulting 1% CH₃CN by volume is regarded as insignificant. Three main products (identified and quantified by HPLC) are formed: 16-ArOH, 16-ArBr, and 16-ArH. The first two products (the ones of primary interest) arise from heterolytic C/N cleavage and trapping of 16-ArN₂⁺ by Br⁻ or H₂O, Scheme 2. The 16-ArH product (and the unidentified OX product) is formed in an unwanted redox reaction between 16-ArN₂⁺ and 16-ArOH. We corrected for the consumption of 16-ArOH to obtain normalized product yields, %16-ArBr₁ and %16-ArOH₁, from the just the heterolytic reaction and carried out a series of control experiments to demonstrate the validity of the correction (see below).

Results

Table 1 lists HPLC results for 1.5–5 mM 12-2-12 2Br in 0.1 mM HBr including peak areas, measured, and normalized product yields. Results for 12-3-12 2Br and 12-4-12 2Br are in the Supporting Information. These normalized product yields depend on both the selectivity of the heterolytic dediazonation

(47) Romsted, L. S.; Zhang, J.; Cuccovia, I. M.; Politi, M. J.; Chaimovich, H. *Langmuir* **2003**, *19*, 9179–9190.

(48) Romsted, L. S. Snared by Trapping: Chemical Explorations of Interfacial Compositions of Cationic Micelles. In *Adsorption and Aggregation of Surfactants in Solution*; Mittal, K. L., Shah, D. O., Eds.; Marcel Dekker: New York, 2002; pp 149–170.

(49) Cuccovia, I. M.; Romsted, L. S.; Chaimovich, H. *J. Colloid Interface Sci.* **1999**, *220*, 96–102.

(50) Chaudhuri, A.; Loughlin, J. A.; Romsted, L. S.; Yao, J. *J. Am. Chem. Soc.* **1993**, *115*, 8351–8361.

(51) Geng, Y.; Romsted, L. S. *J. Phys. Chem. B* in press.

Table 1. HPLC Peak Areas, Observed Yields, and Normalized Yields for Reaction of 0.1 mM 16-ArN₂⁺ in Aqueous 12-2-12 2Br Gemini Micellar Solutions from 1.5 mM to 5 mM with [HBr] = 0.1 mM at 25 °C M^a

[12-2-12] mM	peak areas (10 ⁵ μV·s) ^b			observed yields (%)				normalized yields (%) ^c	
	16-ArOH	16-ArH	16-ArBr	16-ArOH	16-ArH	16-ArBr	total ^c	16-ArOH _I	16-ArBr _I
1.5	1.878	7.474	4.091	8.70	36.1	13.4	94.3	77.0	23.0
1.7	2.956	6.651	4.328	13.7	32.1	14.2	92.1	76.4	23.6
1.9	2.264	7.132	4.290	10.5	34.4	14.0	93.4	76.2	23.8
2.0	2.109	7.319	4.359	9.76	35.4	14.3	94.7	76.0	24.0
2.1	3.080	6.745	4.825	14.3	32.6	15.8	95.2	74.8	25.2
2.3	2.935	6.339	5.439	13.6	30.6	17.8	92.6	71.3	28.7
2.5	2.185	6.621	5.727	10.1	31.9	18.7	92.8	69.2	30.8
2.7	2.639	6.386	6.114	12.2	30.8	20.0	93.9	68.3	31.7
3.0	2.961	6.129	6.232	13.7	29.6	20.4	93.3	68.0	32.0
3.5	4.059	5.561	6.632	18.8	26.9	21.7	94.2	67.8	32.2
4.0	3.196	5.881	6.328	14.8	28.4	20.7	92.3	67.6	32.4
5.0	2.871	6.143	6.385	13.3	29.7	20.9	93.5	67.3	32.7

^a Reaction time ca. 16 h to ensure the complete dediazonation reaction. 16-ArN₂BF₄ prepared as a 10 mM stock solution in MeCN. ^b 100 μL sample injections. Peak areas are average of three injections. ^c See Scheme 3 for definitions of total observed yields and normalized yields.

reaction toward bromide ion and water and their interfacial concentrations in the interfacial region of 12-2-12 2Br micelles. The selectivities and product yields were used to estimate interfacial molarities of Br_m and H₂O_m and their molar ratios, H₂O_m/Br_m, plotted in Figure 1 by the following process.

In the chemical trapping method, the selectivity of the dediazonation reaction of 16-ArN₂⁺ with Br⁻ and H₂O in the interfacial region of micelles, S_w^{Br}, is assumed to be the same as that for its water-soluble short chain analogue, 1-ArN₂⁺, in an aqueous reference solution of identical composition, eq 1. S_w^{Br} is obtained from chemical trapping product yield ratios of

$$S_w^{\text{Br}} = \frac{[\text{H}_2\text{O}](\% \text{ 1-ArBr})}{[\text{Br}](\% \text{ 1-ArOH})} = \frac{\text{H}_2\text{O}_m(\% \text{ 16-ArBr}_I)}{\text{Br}_m(\% \text{ 16-ArOH}_I)} \quad (1)$$

(% 1-ArBr)/(% 1-ArOH) in 0.01 to 1.75 M aqueous solutions of the bolaform electrolyte, bis(trimethyl)-α,ω-alkanediammonium dihalides, 1-*n*-1 2Br (*n* = 2–4). These chemical trapping results in bolaform electrolyte solutions are published separately.⁵¹ In eq 1, square brackets, [], indicate molarity as determined from weights of 1-*n*-1 2Br and water in volumetric flasks. The stoichiometric concentration of Br⁻, [Br], is twice the molarity of the bolaform electrolyte. Measured S_w^{Br} values decrease from about 16 to 3 as the concentration of Br⁻ increases from 0.02 to 3.5 M but are only slightly dependent upon spacer length.⁵¹ Equation 1 shows that at a particular S_w^{Br} value, when the yield ratio from reaction in a gemini micellar solution with a particular spacer length, e.g., *n* = 2, is the same as the yield ratio in an aqueous bolaform electrolyte solution with the same spacer length, then H₂O_m/Br_m = [H₂O]/[Br]. To estimate Br_m, we make the corollary assumption that *when the yields are the same, the concentrations are the same.* For example, if we obtain a 40% yield of 16-ArBr_I in a solution of 12-2-12 2Br, then Br_m = [Br] when the yield of 1-ArBr is 40% in an aqueous solution of 1-2-1 2Br. In practice, plots of % 1-ArBr versus [Br] in 1-*n*-1 2Br (*n* = 2–4) solutions are used as standard curves for product yields obtained in 12-*n*-12 2Br (*n* = 2–4) micelles.^{2,50,51} Values of H₂O_m are calculated from normalized % 16-ArOH_I and % 16-ArBr_I yields and the corresponding S_w^{Br} value in the bolaform electrolyte solution using eq 1. Note that the volume of the interfacial region need not be known to estimate Br_m and H₂O_m. The Br_m and H₂O_m values and H₂O_m/Br_m ratios for all three surfactants are plotted in Figure 1.

The measured 16-ArH values were included quantitatively in the calculation of normalized product yields, 16-ArOH_I and

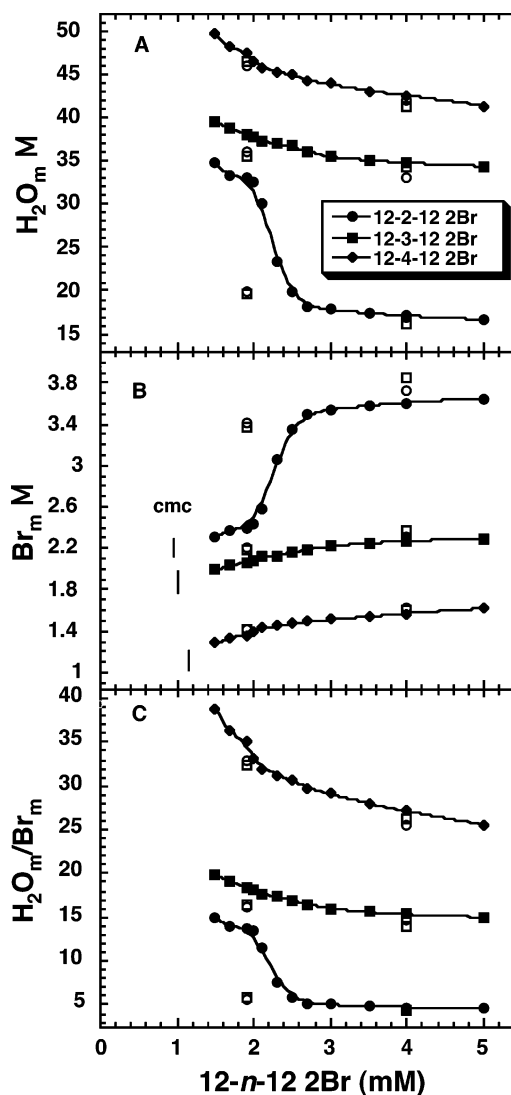


Figure 1. Interfacial Br⁻, Br_m (B) and water, H₂O_m (A) molarities and H₂O_m/Br_m molar ratios (C) in 12-*n*-12 2Br (*n* = 2–4) gemini micelles at 25 °C with 0.1 mM HBr. The vertical lines are literature cmc values (see text). The open symbols at 1.9 and 4 mM 12-*n*-12 surfactant contain 1 mM HBr (○) and 1 mM NaBr and 0.1 mM HBr (□).

16-ArBr_I, which come from the heterolytic dediazonation reaction, using the process and equations summarized in Scheme 3. The oxidation/reduction reaction between 16-ArN₂⁺ and 16-ArOH decreases the 16-ArOH yield by an amount equal to the

Scheme 3. Equations Used to Determine Normalized Product Yields %16-ArBr_I and %16-ArOH_I

The total yield of arenediazonium ion consumed in two reactions:

$$\%16\text{-ArN}_2^+_{\text{T}} = \%16\text{-ArN}_2^+_{\text{h}} + \%16\text{-ArN}_2^+_{\text{Ox/Red}} \quad (2)$$

Amount of arenediazonium ion consumed in the heterolytic pathway:

$$\%16\text{-ArN}_2^+_{\text{h}} = \%16\text{-ArOH}_{\text{h}} + \%16\text{-ArBr}_{\text{h}} \quad (3)$$

Amount of arenediazonium ion consumed in the oxidation/reduction pathway:

$$\%16\text{-ArN}_2^+_{\text{Ox/Red}} + \%16\text{-ArOH}_{\text{Ox/Red}} = \%16\text{-ArH}_{\text{Ox/Red}} + \%16\text{-OX}_{\text{Ox/Red}} \quad (4)$$

Equation 4 shows that each equivalent of 16-ArH produced represents the loss of one equivalent

of 16-ArOH and one of 16-ArN₂⁺. Thus, %16-ArN₂⁺_T is given by:

$$\%16\text{-ArBr}_{\text{h}} + \%16\text{-ArOH}_{\text{h}} + 2(\%16\text{-ArH}_{\text{Ox/Red}}) = \%16\text{-ArN}_2^+_{\text{T}} \quad (5)$$

where $2(\%16\text{-ArH}_{\text{Ox/Red}}) = \%16\text{-ArOH}_{\text{Ox/Red}} + \%16\text{-ArH}_{\text{Ox/Red}}$. %16-ArBr_h + %16-ArOH_h are the observed yields of these products listed in Table 1.

The total product yield from only the heterolytic pathway:

$$\%16\text{-ArOH}_{\text{h}} + \%16\text{-ArH}_{\text{Ox/Red}} + \%16\text{-ArBr}_{\text{h}} = \%16\text{-ArN}_2^+_{\text{h}} \quad (6)$$

where %16-ArH_{Ox/Red} = %16-ArOH_{Ox/Red} = the observed %16-ArH yield in Table 1.

Definitions of normalized product yields:

$$\%16\text{-ArBr}_I = \frac{100(\%16\text{-ArBr}_{\text{h}})}{\%16\text{-ArN}_2^+_{\text{h}}} \quad (7)$$

$$\%16\text{-ArOH}_I = \frac{100((\%16\text{-ArOH}_{\text{h}}) + (\%16\text{-ArH}_{\text{Ox/Red}}))}{\%16\text{-ArN}_2^+_{\text{h}}} \quad (8)$$

where subscripts T = total, h = heterolytic, Ox/Red = Oxidation/Reduction, and I = normalized yield.

16-ArH yield, and the sum of the 16-ArBr, 16-ArOH, and 16-ArH yields, eq 6, is the total yield from just the heterolytic reaction. A typical example illustrates the effect of this correction. The observed HPLC yields in 1.5 mM 12-2-12 2Br (Table 1) of 8.7% 16-ArOH, 36.1% 16-ArH, and 13.4% 16-ArBr were converted into normalized yields of 77.0% 16-ArOH_I and 23.0% 16-ArBr_I. These two yields reflect the selectivity of the heterolytic dediazonation reaction with water and bromide ion. Equations 7 and 8 were used to estimate 16-ArOH_I and 16-ArBr_I for all three gemini surfactants at each surfactant concentration.

A set of control experiments at a higher, but constant, Br⁻ concentration and at two different acidities were carried out to test the validity of the process and equations in Scheme 3. Increasing the solution acidity slows the redox reaction of arenediazonium ions and phenols^{52,53} and should reduce the yield of 16-ArH and increase the yield of 16-ArOH. Increasing the stoichiometric Br⁻ concentration to 1 mM should have little effect on Br_m because Br_m is ca. 1 M or greater, provided the micelles do not change structure (see below). Table 2 lists trapping results for the three geminis at two concentrations (1.9

and 4 mM). These two concentrations were deliberately selected to lie below and above the sigmoidal transition for 12-2-12 2Br in Figure 1. For all three geminis, increasing [H⁺] from 0.1 mM HBr (Table 1) to 1 mM (Table 2A and C) dramatically reduces the yield of 16-ArH at both 1.9 mM and 4 mM amphiphile concentration, and the yields of both 16-ArOH and 16-ArBr increase substantially (compare with results for 1.9 mM 12-2-12 2Br in Table 1). Adding 1 mM NaBr (Tables 2B and 2D) at 0.1 mM HBr gives %16-ArH yields that are similar to those in Table 1, also at 0.1 mM HBr, but in the absence of added NaBr. The normalized yields %16-ArBr_I and %16-ArOH_I at 1.9 mM and 4 mM gemini are almost the same in 0.1 mM Br (Table 1) and in 1 mM HBr and NaBr (Table 2), except for the results in 1.9 mM 12-2-12 2Br. In 1.9 mM 12-2-12 2Br and 0.1 mM HBr, the 16-ArOH_I/16-ArBr_I ratio is 76.2/23.8 (Table 1). In contrast, in 1.9 mM 12-2-12 2Br at both 1 mM HBr and 1 mM NaBr, the ratio decreases to 69/31. Given the high consistency of the data for all three geminis, this yield ratio change is substantial and can be attributed to rod formation that favors bromide product (see Discussion). The H₂O_m and Br_m molarities and H₂O_m/Br_m ratios calculated from the normalized product yields obtained in the control experiments are plotted in Figure 1.

(52) Romsted, L. S.; Yao, J. *Langmuir* **1996**, *12*, 2425–2432.

(53) Brown, K. C.; Doyle, M. P. *J. Org. Chem.* **1988**, *53*, 3255.

Table 2. Observed and Normalized Yields for Dediazonation of 0.1 mM 16-ArN₂⁺ in 12-2-12 2Br, 12-3-12 2Br, and 12-4-12 2Br Gemini Micellar Solutions at 25 °C^a

gemini	peak areas (10 ⁵ μV·s) ^b			observed yields (%)				normalized yields (%) ^c	
	16-ArOH	16-ArH	16-ArBr	16-ArOH	16-ArH	16-ArBr	total ^c	16-ArOH _i	16-ArBr _i
A. In 1.9 mM gemini surfactant and 1 mM HBr									
12-2-12	11.619	1.243	8.249	53.8	6.00	27.0	92.8	68.9	31.1
12-3-12	13.799	0.620	6.674	63.9	2.99	21.8	91.7	75.4	24.6
12-4-12	15.232	0.443	5.625	70.5	2.14	18.4	93.2	79.8	20.2
B. In 1.9 mM gemini surfactant, 1 mM NaBr and 0.1 mM HBr									
12-2-12	2.636	6.274	5.812	12.2	30.3	19.0	91.8	69.1	30.9
12-3-12	6.965	4.541	5.318	32.2	21.9	17.4	93.4	75.7	24.3
12-4-12	6.823	4.838	4.307	31.6	23.4	14.1	92.5	79.6	20.4
C. In 4 mM gemini surfactant and 1 mM HBr									
12-2-12	12.256	0.560	9.033	56.7	2.70	29.5	91.7	66.8	33.2
12-3-12	14.293	0.329	7.018	66.2	1.59	22.9	92.3	74.7	25.3
12-4-12	14.883	0.213	6.281	68.9	1.03	20.5	91.5	77.3	22.7
D. In 4 mM gemini surfactant, 1 mM NaBr and 0.1 mM HBr									
12-2-12	2.392	6.315	6.521	11.1	30.5	21.3	93.4	66.1	33.9
12-3-12	6.851	4.398	5.659	31.7	21.2	18.5	92.7	74.1	25.9
12-4-12	10.615	2.739	5.499	49.2	13.2	18.0	93.6	77.6	22.4

^a See Table 1 for details on footnotes a–c.

Discussion

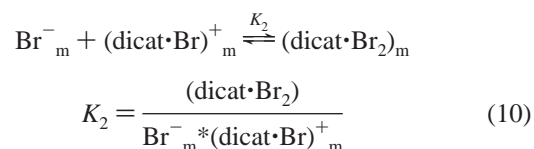
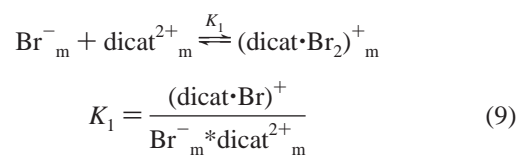
The interfacial concentrations of Br[−] and H₂O are expressed in molarities because interfacial molarities are the same as the molarities of an aqueous reference solution. Put differently, when the forces determining micelle morphology are in balance, their interfacial compositions are modeled with an aqueous salt solution having the same molarities of counterion and water. When the balance of forces shifts because the solution composition is changed, the interfacial molarities change, and the product yields from reaction with 16-ArN₂⁺ correspond to product yields from reaction of 1-ArN₂⁺ in an aqueous reference solution of different composition.

The most striking features of the results in Figure 1 are the marked increase in Br_m, the concomitant decrease in H₂O_m, the drop in the H₂O_m/Br_m molar ratio for 12-2-12 2Br, and the absence of such transitions for 12-3-12 2Br and 12-4-12 2Br micellar solutions. Of these three gemini amphiphiles, only 12-2-12 2Br is reported to form rods just above its cmc at 25 °C.³⁴ The initial Br_m molarities are highest for 12-2-12 2Br, ca. 2.4 M, and lowest for 12-4-12 2Br, ca. 1.3 M. Values of H₂O_m show complementary changes. The sigmoidal changes in Br_m and H₂O_m for 12-2-12 2Br but their absences for the other two geminis are a direct consequence of changes in 16-ArBr and 16-ArOH product yields (and HPLC peak areas) and do not depend on assumptions about the selectivity of the reaction or the effect of the competing reaction producing 16-ArH (see Table 1 and Supporting Information). In solutions of all three gemini micelles, product yields depend on the average concentrations of H₂O and Br[−] in the interfacial region, not their stoichiometric concentrations in bulk solution. The total yield must be 100%, and if the yield of 16-ArBr increases, that of 16-ArOH must decrease. The marked product yield (and peak area) changes were only observed for 12-2-12 2Br.

Figure 1C shows not only that the H₂O_m/Br_m molar ratios decrease with decreasing spacer length and the ratio for 12-2-12 2Br drops from ca. 15 to about 5 above 3 mM 12-2-12 2Br, but also that the ratios for the other two amphiphiles are higher and decrease only gradually. A H₂O_m/Br_m molar ratio of 5 is about the same as reported hydration numbers of Br[−] itself,¹³ which means that not all the amphiphile headgroups and

interfacial Br[−] can be fully hydrated in rodlike micelles and that sphere-to-rod transition is accompanied by substantial dehydration of the 12-2-12 2Br micellar interface. At 5 mM 12-3-12 2Br and 12-4-12 2Br, the H₂O_m/Br_m molar ratios are about 15 and 26, respectively, indicating that their headgroups and counterions are 3 to 5 times more hydrated than those of 12-2-12 2Br and probably too hydrated to form rods, although significantly increasing the [12-3-12 2Br] probably leads to rods³⁴ and adding a significant amount of NaBr may induce the transition in either surfactant. However, adding 1 mM Br[−] is not sufficient to induce rod formation by 12-3-12 2Br or 12-4-12 2Br, Figure 1, open points. Increasing [Br[−]] 10-fold, from 0.1 mM to 1 mM by adding HBr or NaBr, has little effect on Br_m and H₂O_m, except at 1.9 mM 12-2-12 2Br. The substantial increase in Br_m and decrease in H₂O_m in 1.9 mM 12-2-12 2Br with 1 mM added Br[−] compared to 0.1 mM HBr is consistent with added Br[−] inducing the formation of rodlike micelles by 12-2-12 2Br, but 12-3-12 2Br or 12-4-12 2Br micelles remain spherical.

Product yields obtained by chemical trapping were used to estimate the interfacial concentrations of free and paired headgroups and counterions and their fractions expressed in terms of interfacial Br[−] molarity, Br_m. The equilibria describing the formation of the first and second ion pairs are given by eqs 9 and 10:



where the asterisk (*) indicates multiplication and the other symbols are shown in Scheme 2. Equations 9 and 10 are combined with mass balance equations and solved to obtain a

Scheme 4. Equations and Values of Parameters Used to Calculate Interfacial Concentrations and Fractions of Free and Paired Ions in the Interfacial Regions of Gemini Micelles

Mass balance equations:

$$\text{Br}_m = \text{Br}_m^- + (\text{dicat} \cdot \text{Br})_m^+ + 2(\text{dicat} \cdot \text{Br}_2)_m \quad (11)$$

$$\text{dicat}_m = \text{dicat}^{2+}_m + (\text{dicat} \cdot \text{Br})_m^+ + (\text{dicat} \cdot \text{Br}_2)_m \quad (12)$$

$$\text{Br}_m = (2 \cdot \text{dicat}_m / \beta) + 0.0001 \text{ M HBr} \quad (13)$$

$$\text{Br}_m = \text{Br}_m^- + (\text{dicat} \cdot \text{Br})_m^+ + 2 \cdot (\text{dicat} \cdot \text{Br}_2)_m \quad (14)$$

$$\text{dicat}_m = \text{dicat}^{2+}_m + (\text{dicat} \cdot \text{Br})_m^+ + (\text{dicat} \cdot \text{Br}_2)_m \quad (15)$$

Cubic equation for Br_m^- :

$$K_1 \cdot K_2 \cdot (\text{Br}_m^-)^3 + (K_1 + 2 \cdot K_1 \cdot K_2 \cdot \text{dicat}_m - K_1 \cdot K_2 \cdot \text{Br}_m) \cdot (\text{Br}_m^-)^2 + (1 + K_1 \cdot \text{dicat}_m - K_1 \cdot \text{Br}_m) \cdot \text{Br}_m^- - \text{Br}_m = 0 \quad (16)$$

Equations for fractions of free and paired ions used for plots in Figure 2:

$$\text{fraction of free interfacial bromide ion: } \text{Br}_f^- = \frac{\text{Br}_m^-}{\text{Br}_m} \quad (17)$$

$$\text{fraction of monobromo-dication pair: } (\text{dicat} \cdot \text{Br})_f^+ = \frac{(\text{dicat} \cdot \text{Br})_m^+}{\text{Br}_m} \quad (18)$$

$$\text{fraction of dibromo-dication pair: } (\text{dicat} \cdot \text{Br}_2)_f = \frac{(\text{dicat} \cdot \text{Br}_2)_m}{\text{Br}_m} \quad (19)$$

$$\text{fraction of free dication: } \text{dicat}_f^{2+} = \frac{2 \cdot \text{dicat}^{2+}_m}{\text{Br}_m} \quad (20)$$

fraction of positive (+) charge on gemini head groups:

$$+\text{charge}_f = \frac{(2 \cdot \text{dicat}^{2+}_m + (\text{dicat} \cdot \text{Br})_m^+)}{((2 \cdot \text{dicat}^{2+}_m + (\text{dicat} \cdot \text{Br})_m^+ + (\text{dicat} \cdot \text{Br}_2)_m))} \quad (21)$$

Association Constants and β :

$K_1 = 16.7$ (12-2-12 2Br), 5.79 (12-3-12 2Br), 1.75 (12-4-12 2Br), $K_2 = 0.83$ for all three gemini

amphiphiles, $\beta = 0.8$.

cubic equation for Br_m^- , Scheme 4. The factor 2 appears in some equations because each equivalent of gemini amphiphile added gives 2 equiv of Br^- . Details on the derivation of the cubic equation and the equations for calculating the concentrations of dicat^{2+}_m , $(\text{dicat} \cdot \text{Br})_m^+$, and $(\text{dicat} \cdot \text{Br}_2)_m$ are in the Supporting Information.

The solution to the cubic equation to obtain Br_m^- at each 12-*n*-12 2Br (*n* = 2–4) concentration requires the following: (a) the measured values of Br_m ; (b) the concentrations of dicat_m obtained from eq 13 (Scheme 4); the assumptions that (c) the cmc (ca. 0.001 M) is much smaller than dicat_m molarity (≥ 1 M); (d) the degree of counterion binding, β , is constant; and (e) values for K_1 and K_2 . Values of β are obtained from α ($\beta = 1 - \alpha$). The experimental values of α are method (and investigator) dependent, and the variation in α by different methods is often as great as the variation with compositional variables such as counterion type, temperature, and surfactant chain length.^{54–56} Different experimental methods give different estimates of α for micelles of these gemini amphiphiles and variations in the experimental estimates of α are often greater

than the variation with some particular micellar property (e.g., counterion type),⁵⁶ and β for the three gemini surfactants is constant to within about 10%, i.e., $\beta \approx 0.8 \pm 0.1$. Because the value of β is near one (1), small variations in its value should not significantly affect the calculated molarities of the free and paired ions in the interfacial region, and for simplicity we assumed $\beta = 0.8$ for all three gemini amphiphiles and independent of surfactant concentration. An approach developed by Zana and Bales based on EPR⁵⁷ and NMR⁵⁸ methods is consistent with α (and therefore β) remaining constant with added surfactant and counterion, but the aggregation number increases.

The values for K_1 and K_2 , listed in Scheme 4, are measured association constants for the binding of the first and second Br^- in aqueous 1-*n*-1 2Br (*n* = 2–4) salt solutions with the same spacer length.⁵¹ The association constants were estimated from chemical trapping in aqueous solutions of bolaform electrolytes, 1-*n*-1 2Br (*n* = 2–4) and confirmed by ⁷⁹Br NMR line width experiments. Values of K_1 for the binding of the first Br^- to 1-*n*-1 (*n* = 2–4) dications were obtained by iterative fits of % 1-*n*-1 yields and ⁷⁹Br line widths as a function of bolaform electrolyte concentration. Values of K_2 were obtained by

(54) Gunnarsson, G.; Jonsson, B.; Wennerstrom, H. *J. Phys. Chem.* **1980**, *84*, 3114–3121.

(55) Kresheck, G. C. Surfactants. In *Water: A Comprehensive Treatise: Aqueous Solutions of Amphiphiles and Macromolecules*; Franks, F., Ed.; Plenum Press: New York, 1975; Vol. 4, pp 95–167.

(56) Romsted, L. S. *Rate Enhancements in Micellar Systems*. Ph.D., Indiana University, 1975.

(57) Tcacenco, C. M.; Zana, R.; Bales, B. L. *J. Phys. Chem. B* **2005**, *109*, 15997–16004.

(58) Paul, A.; Griffiths, P. C.; Pettersson, E.; Stilbs, P.; Bales, B. L.; Zana, R.; Heenan, R. K. *J. Phys. Chem. B* **2005**, *109*, 15755–15779.

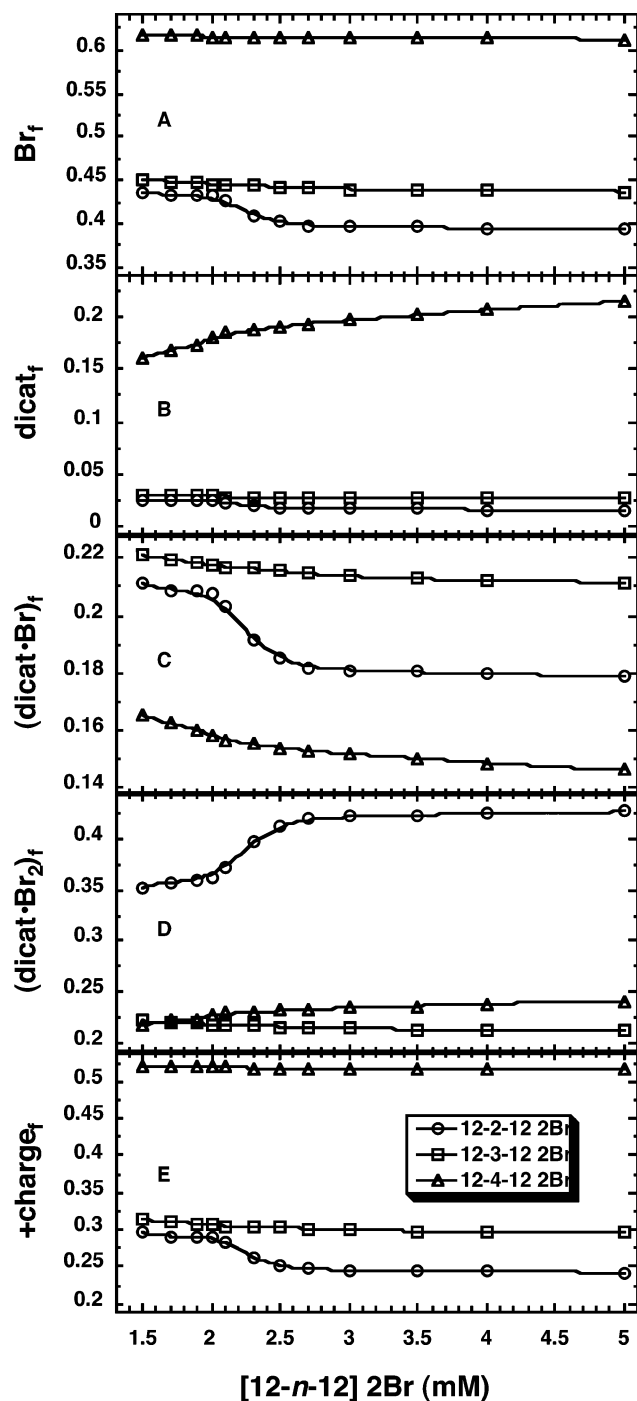


Figure 2. Fractions of: free ions, Br_f (A) and dicat_f (B); paired ions, $(\text{dicat}\cdot\text{Br})_f$ (C) and $(\text{dicat}\cdot\text{Br}_2)_f$ (D); and the fraction of net positive (+) charge, $+\text{charge}_f$, (E) on the gemini headgroups in micellar solutions of 12- n -12 2Br ($n = 2$ –4) in 0.1 mM HBr at 25 °C.

assuming that binding of the second Br^- to the dication is the same as that for association of Br^- and the tetramethylammonium cation (TMA^+). This equivalence is supported by the fact that the dependence of both % 1- n -12 2Br yields and ^{79}Br line widths on 1- n -12 2Br concentration and TMA^+ at high stoichiometric Br^- concentration ($>0.2\text{ M}$).⁵¹

The results in Figures 1 and 2 illustrate the relationship between the changes in ion specific interactions with changes in amphiphile headgroup structure and the sphere-to-rod transition. The interfacial compositions of gemini micelles are, in essence, like those of mixed micelles composed of dicationic,

monocationic, and zwitterionic headgroups, Scheme 2. The fraction of each form present depends on spacer length, the concentration of added Br^- , the strength of counterion specific interactions with the headgroup, and the free energies of hydration of the counterion and each type of headgroup, which can be ranked in the order: $\text{dicat}^{2+}_m > (\text{dicat}\cdot\text{Br})^+_m > (\text{dicat}\cdot\text{Br}_2)_m$. Thus, the average molarities of Br^- and water within the interfacial region, Br_m and H_2O_m (and the $\text{H}_2\text{O}_m/\text{Br}_m$ molar ratio), Figure 1, depend on the degree of ion pairing, which depends on headgroup spacer length.

The fractions of each form present in the micellar interfaces of the 12- n -12 2Br ($n = 4$) amphiphiles illustrate this point clearly. When $n = 4$, the association constant is small, $K_1 = 1.75$, the fractions of paired headgroups (Figure 2C and 2D) are the lowest, the fractions of free ions are the highest (Figure 2A and 2B), and the net + charge on the headgroups is the highest (Figure 2E). When $n = 3$, $K_1 = 5.79$, there is a significant decrease in the fractions of free ions, a concomitant increase in the fractions of paired ions, and the net + charge drops from about 0.5 to 0.3. When $n = 2$, $K_1 = 16.7$, the fractions of free ions are the smallest, the fraction of $(\text{dicat}\cdot\text{Br}_2)_f$ increases and the fraction of $(\text{dicat}\cdot\text{Br})_f$ decreases significantly above 2 mM 12- n -12 2Br compared to the gemini amphiphile ($n = 3$), and the net + charge drops to about 0.23. This transition is accompanied by a large decrease in interfacial hydration, Figure 1, and suggests that $(\text{dicat}\cdot\text{Br}_2)_m$ is almost completely dehydrated because ion pairs are less strongly hydrated than free ions.¹⁴ However, the $(\text{dicat}\cdot\text{Br})^+$ pair is probably substantially more hydrated as indicated by the $\text{H}_2\text{O}_m/\text{Br}_m$ molar ratios for 12-3-12 2Br compared to 12-2-12 2Br. In summary, as the extent of ion pairing increases, the net degree of hydration of the free amphiphile headgroups and counterions and their pairs decreases. Ion pairing is enhanced by shortening the spacer length of the gemini amphiphiles, by increasing [12-2-12 2Br] and, we postulate, by adding Br^- (1.9 mM 12-2-12 2Br). Interfacial hydration of single chain surfactant micelles has also been estimated by using an ESR probe method,⁵⁷ and effective interfacial water concentrations have been obtained from spectral shifts of solvatochromic probes.⁵⁹ The results are consistent with those obtained here.

In the interfacial specific ion-pairing/hydration model, the determining characteristic of aggregate morphology is not molecular packing per se but the balance of free energies between the hydrophobic effect and short range, specific headgroup-counterion pair and ion hydration interactions. Aggregate growth stops because the stronger free energies of hydration of the surfactant headgroups and counterions provide balance. All the water hydrating headgroups and counterions is considered part of the micelle. The balancing force within the interfacial region depends on headgroup and counterion types and their interfacial concentrations. Free headgroups and counterions are more strongly hydrated than headgroup-counterion pairs,¹⁴ but changes in amphiphile headgroup structure or counterion type and concentration that promote an increase in their interfacial concentrations also promote ion pair formation, which reduces the total free energy of hydration per surfactant monomer and permits the release of interfacial water. The entropy of the system increases and the free energy of

(59) Tada, E. B.; El Seoud, O. A. *Prog. Colloid Polym. Sci.* **2002**, *121*, 101–109.

micellization becomes more negative.⁶ The small energy bill per surfactant monomer for forming headgroup-counterion pair and the release of water of hydration is paid by the hydrophobic effect, just as the energy bill for micelle formation per monomer is paid for by the small (<1 kcal/mol) free energy of transfer per methylene from water to the micellar core.⁶⁰ However, the total free energy per micelle is much larger owing to the release of ordered water from a multitude of methylenes during micellization, so the total free energy change for ion pairing per aggregate can be substantial because of the release of water when rodlike micelles are formed.

The interfacial specific ion-pairing/hydration model also explains the sphere-to-rod transitions of single chain cetyltrimethylammonium, CTA⁺, amphiphiles. The sphere-to-rod transitions of CTABr and CTACl occur at ca. 0.1 M Br⁻ and ca. 1.0 aqueous Cl⁻, respectively, as do their increases in interfacial counterion and decreases in interfacial water concentrations.³ In an example of surprising counterion sensitivity, micelles of CTA⁺ amphiphiles with 3,5-dichlorobenzoate, but not 2,6-dichlorobenzoate counterions, show concomitant sphere-to-rod and interfacial counterion and water transitions.¹

This model is essentially the same as the one used to describe the balance of forces controlling micellization of nonionic amphiphiles, i.e., the hydrophobic effect driving aggregation is balanced by the free energy of hydration of the headgroups, often polyoxyethylene chains or sugar groups.⁶ The model should also be applicable to specific salt effects on zwitterionic micelles and mixtures of amphiphiles with different ion pair and headgroup and counterion hydration free energies. Zwitterionic amphiphiles, which are conceptually similar to the uncharged form of the gemini amphiphile, (dicat·Br₂), are the most poorly hydrated of the charged headgroups, exert a weaker balancing force, and have lower cmc's.⁶ However, like ionic micelles, the properties of zwitterionic amphiphiles such as sulfobetaines show a substantial dependence on the type of anion added as salt, with the largest, most polarizable anions having the biggest effect.^{49,61}

The interfacial specific ion-pairing/hydration model provides a conceptual alternative to the packing parameter. The packing parameter, N_S , is given by

$$N_S = \frac{V}{al} \quad (22)$$

where V is the volume of the hydrophobic chain of the amphiphile, a is its cross sectional area at the headgroup, and l is the length of its hydrocarbon tail.^{25,26,62,63} The basic assumption in estimating the packing parameter is that amphiphiles of a particular geometry, e.g., cones, cylinders, inverse cones, will pack optimally (fill the geometrical space) in a particular aggregate shape. For example, the packing parameter, N_S , is $1/3$ for spherical micelles, $1/3-1/2$ for cylindrical micelles, $1/2-1$ for vesicles, and ca. 1 for planar bilayers. These changes in the packing parameter provide a qualitative feel for the idea

that single chain amphiphiles such as CTABr or SDS tend to form spherical aggregates because the headgroup has a larger cross sectional area than its tail, whereas twin tail amphiphiles such as phospholipids have a more cylindrical geometry with the headgroups and tails having similar cross sectional areas and they pack better into rods, vesicles, and bilayers. However, the weakness of the packing parameter approach is that it does not account for the shift in balance of forces controlling aggregate morphology with the structures of ionic amphiphiles. For example, twin tail amphiphiles form spherical micelles when the tails are relatively short, e.g., gemini amphiphiles³⁴ or short chain phospholipids.⁶⁴ Also, single chain amphiphiles undergo sphere-to-rod transitions, and the concentration at which the sphere-to-rod transition occurs (the second cmc) depends on amphiphile chain length, counterion type,^{1,3,6-11,41,43,48} and temperature.⁶

The packing parameter approach does not account for the dependence of morphology on amphiphile structure (and amphiphile and counterion concentration) because it contains no method for defining the cross sectional area of the amphiphile headgroup. For example, the radius or thickness of a particular aggregate shape correlates reasonably well with l , but that shape is the same for all values of l . In eq 22, the value of N_S for a spherical micelle is independent of l because both the numerator, the volume of a cone, $V = 1/3(\pi a^2 l)$, and the denominator depend on l and the dependence cancels. Thus, the packing parameter does not predict the frequently observed tendency of amphiphiles to form rodlike aggregates at lower amphiphile concentrations with increasing chain length. In summary, specific ion effects on morphological transitions of ionic surfactants cannot be treated because eq 22 contains no term for specific headgroup-counterion and hydration interactions.

Finally, the interfacial specific ion-pairing/hydration model suggests that the small variations in measured α values for many different surfactant systems mean that α values reflect the net balance of long-range Coulombic attractions between counterions in the bulk aqueous phase and a charged aggregate surface (outside of the interfacial region), which are not very sensitive to surfactant chain length, counterion type, and temperature.⁵⁴⁻⁵⁶ Thus the net surface charge density of micelles does not make a significant contribution to micelle formation or morphology, i.e., the first and second cmc's, because they are sensitive to surfactant chain length, counterion type, and temperature. Aggregate formation and morphology do not depend on headgroup repulsions but on the balance of the hydrophobic effect and specific headgroup and counterion and hydration interactions within the interfacial region.

Conclusions

Chemical trapping results in 12- n -12 2Br ($n = 2-4$) gemini amphiphiles provide strong evidence that the sphere-to-rod transition of 12-2-12 2Br, but not micelles of 12-3-12 2Br and 12-4-12 2Br, is driven by concomitant ion pair formation and release of water of hydration from the interfacial region because ion pairs are less strongly hydrated than free ions. These and other chemical trapping results support an interfacial specific ion-pairing/hydration model for headgroups and counterions within the micellar interface. The model provides a qualitative

(60) Tanford, C. *The Hydrophobic Effect: Formation of Micelles and Biological Membranes*, 2nd ed.; Wiley: New York, 1980.

(61) Beber, R. C.; Bunton, C. A.; Savelli, G.; Nome, F. *Prog. Colloid Polym. Sci.* **2004**, *128*, 249-254.

(62) Israelachvili, J. N.; Mitchell, D. J.; Ninham, B. W. *J. Chem. Soc., Faraday Trans 2* **1976**, *72*, 1525-1568.

(63) Evans, D. F.; Wennerstrom, H. *The Colloidal Domain: Where Physics, Chemistry, Biology and Technology Meet*; VCH Publishers: New York, 1994.

(64) Jain, M. K. *Introduction to Biological Membranes*, 2nd ed.; John Wiley & Sons: New York, 1988.

explanation for the balancing force to the hydrophobic effect that depends on short range, specific ion-pair and hydration interactions within the interfacial region. It also provides a qualitative explanation for specific counterion effects following a Hofmeister series such as the cmc, the variation in counterion exchange constants, and chemical reactivity. Indeed, the varied structural motifs of micelles and other association colloids (spheres, rods, lamellar, cubic, etc.) depend on the structure and hydrophobicity of the amphiphilic tail(s), as is well-known, but also on specific ion hydration, ion pairing, and the release of water into the aqueous domain. The logic of this model is essentially the same as Eisenman treatment for the interpretation of changes in counterion affinities with the changes in the compositions of glass electrodes¹⁷ and changes in affinity orders reported in biological systems¹⁸ and the effect of increasing cross linking on the ion exchange constants of resins.²²

Acknowledgment. L.S.R. and Y.G. thank Yuan Zhong for crucial assistance with undertaking the calculations of associa-

tion constants and interfacial constants and making sure they are correct, Dr. Jason Keiper for intellectual stimulation, Clifford A. Bunton, J.B.F.N. Engberts, Ron Sauers, Frank Quina, Iolanda Cuccovia, and Hernan Chaimovich for helpful discussions and the National Science Foundation for financial support from the Unimolecular Processes Division (CHE-952606 and CHE-0411990) and International Programs (INT-97-22458) of the National Science Foundation.

Supporting Information Available: The Experimental Section is on pages S3–S5. Tables S1–S5 list HPLC results and estimated interfacial Br^- and H_2O concentrations, and Tables S6–S8 list calculated interfacial concentration and mole fractions of free and paired ions, a derivation of the cubic equation and other equations for estimating interfacial concentrations, and molar fractions. This material is available free of charge via the Internet at <http://pubs.acs.org>.

JA056807E